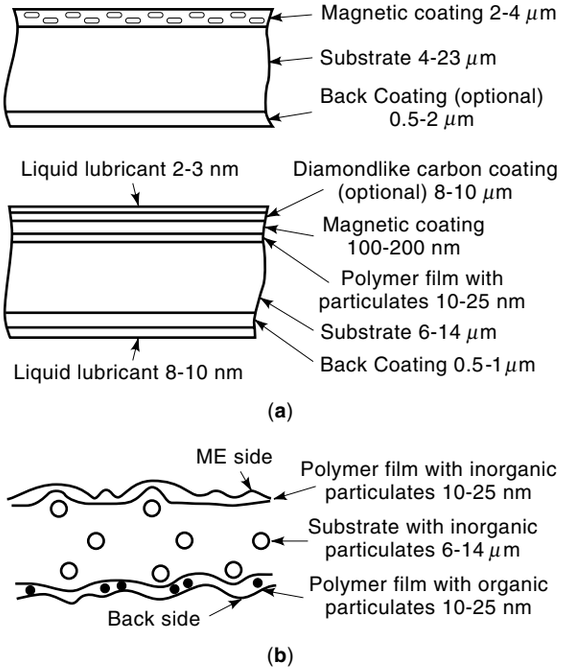

Figure 1. Sectional view of (a) A particulate and a metal-evaporated magnetic tape. (b) A coated PET substrate for ME tapes.

MAGNETIC TAPES

Magnetic tapes can be described as multilayer composite materials consisting of a magnetic layer deposited on to a substrate. There are two basic types of magnetic tapes: (1) particulate tapes where magnetic particles are dispersed in a polymeric matrix and coated onto a polymeric substrate, and (2) thin-film tapes where continuous films of magnetic materials are deposited onto the substrate using vacuum techniques. Cross-sectional views of a particulate and a thin-film tape are shown in Fig. 1. The thin-film tape is commonly referred to as a metal-evaporated (ME) tape since it consists of a coating which is applied using evaporation techniques under vacuum. Currently, particulate tapes are more prevalent than ME tapes. However, as discussed by Bhushan (1–3) requirements for higher recording densities with low error rates have resulted in increased use of smoother, ultrathin ME tapes for digital recording.

DESCRIPTION OF TAPE MATERIALS

Standard and Advanced Substrates

The substrate (or base film) for magnetic tapes is typically a polyester material. Polyethylene terephthalate (PET) film is the most commonly used material, however a new polyester material called polyethylene naphthalate (PEN) is beginning to be used for advanced high-density tapes, such as the DC2120XL tape made by 3M/Imation. Ultrathin aromatic polyamide (ARAMID) substrates have been used for Sony NTC-90 microcassettes, and advanced polymers such as polyimides (PI) and polybenzoxazole (PBO) have been studied for their potential as substrates. Table 1 provides a list of substrates studied by Weick and Bhushan (4–6), and a list of magnetic tapes that use ultrathin substrates and/or advanced magnetic coatings can be found in Table 2.

Magnetic Coatings

Particulate. The substrate is coated on one side of a tape with a magnetic coating that is typically 1 to 4 μm thick. This coating contains 70 to 80 wt.% (or 43–50 vol.%) submicron and acicular magnetic particles such as γ-Fe_20_3, Co-modified γ-Fe_20_3, CrO_2, or metal particles (MP) for longitudinal recording. Hexagonal platelets of barium ferrite ($BaO \cdot 6Fe_20_3$) have been used for longitudinal recording, and they can be used for perpendicular recording. These magnetic particles are held in polymeric binders such as polyester-polyurethane, polyether-polyurethane, nitrocellulose, poly(vinyl chloride), poly(vinyl alcohol-vinyl acetate), poly(vinylidene chloride), VAGH, phenoxy, and epoxy. To reduce friction, the coating consists of 1 to 7 wt.% of lubricants (mostly fatty acid esters, e.g., tridecyl stearate, butyl stearate, butyl palmitate, butyl myristate, stearic acid, myrstic acid). Finally, the coating contains a cross linker or curing agent (such as functional isocyanates); a dispersant or wetting agent (such as lecithin); and solvents (such as tetrahydrofuran and methyl isobutyl-ketone). In some media, carbon black is added for antistatic protection if the magnetic particles are highly insulating, and abrasive particles (such as Al_2O_3 and Cr_2O_3) are added as a head cleaning agent and to improve wear resistance. The coating is calendered to a root-mean-square (rms) surface roughness of 8 to 15 nm.

For antistatic protection and for improved tracking, most magnetic tapes have a 1 to 3 μm thick backcoating of polyes-

Table 1. List of Substrate Materials for Magnetic Tapes

Material	Chemical Name[a]	Tradename	Manufacturing Method	Supplier	Thickness (μm)	Currently Used?
PET	Polyethylene terephthalate	Mylar A (57DB)	Drawing	Dupont	14.4	Yes
PEN	Polyethylene naphthalate	Teonex	Drawing	Teijin	4.5	Yes
ARAMID	Aromatic polyamide	Mictron TX-1	Casting	Toray	4.4	Yes
PI	Polyimide	Upilex	Casting	Ube	7.6	No
PBO	Polybenzoxazole		Casting	Dow	5.0	No

[a]Chemical structures of the substrate materials can be found in Ref. 6.

ter–polyurethane binder containing a conductive carbon black and TiO_2, typically 10% and 50% by weight, respectively. More information on particulates used for magnetic tapes can be found in Refs. 1–3.

Thin-Film (Metal-Evaporated). Thin-film (also called metal-evaporated or ME) flexible media consist of a polymer substrate (PET or ARAMID) with an evaporated film of Co–Ni (with about 18% Ni) and experimental evaporated/sputtered Co–Cr (with about 17% Cr) (for perpendicular recording, which is typically 100 to 200 nm thick). Electroplated Co and electroless-plated Co–P, Co–Ni–P, and Co–Ni–Re–P have also been explored but are not commercially used. Since the magnetic layer is very thin, the surface of the thin-film media is greatly influenced by the surface of the substrate film. Therefore, an ultrasmooth PET substrate film (rms roughness ~1.5 to 2 nm) is used to obtain a smooth tape surface. A 10 to 25 nm thick precoat composed of a polymer film with additives is generally applied to both sides of the PET substrate to provide controlled topography, Fig. 1(b). The film on the ME treated side generally contains inorganic particulates (typically SiO_2 with a particle size of 100 to 200 nm diameter and areal density of typically 10,000/mm^2). The film on the back side generally contains organic (typically cross-linked polystyrene) particles. The rms and peak-to-valley (P–V) distances of the ME treated side and the backside typically are 1.5 to 2 nm and 15 to 20 nm, and 3 to 5 and 50 to 75 nm, respectively. The polymer precoat is applied to reduce the roughness (mostly P–V distance) in a controlled manner from that of the PET surface, and to provide good adhesion with the ME films. Particles are added to the precoat to control the real area of contact and consequently the friction. A continuous magnetic coating is deposited on the polymer film. The polymer film is wrapped on a chill roll during deposition, which keeps the film at a temperature of 0 to −20°C. $Co_{80}Ni_{20}$ material is deposited on the film by a reactive evaporation process in the presence of oxygen; oxygen increases the hardness and corrosion resistance of the ME film. The deposited film, with a mean composition of $(Co_{80}Ni_{20})_{80}O_{20}$ consists of very small Co and Co–Ni crystallites which are primarily intermixed with oxides of Co and Ni (Feurstein and Mayr (7); Harth et al. (8)). Various inorganic overcoats such as diamondlike carbon (DLC) in about 10 nm thicknesses are usually used to protect against corrosion and wear. A topical liquid lubricant (typically perfluoropolyether with reactive polar ends) is then applied to the magnetic coating and the backside by rolling. The topical lubricant enhances the durability of the magnetic coating, and if no DLC overcoat is present the lubricant also inhibits the highly reactive metal coating from reacting with ambient air and water vapor. A backcoating is also applied to balance stresses in the tape, and for antistatic protection. More information on thin films used for magnetic tapes can be found in Refs. 1–3.

DESIGN CONSIDERATIONS FOR DEVELOPMENT OF ADVANCED ULTRATHIN MAGNETIC TAPES

The thinner substrates shown in Table 1 allow for a higher volumetric density when a magnetic tape is wound onto a reel. To achieve this higher volumetric density, the product of the linear and track densities must also be high. This product is commonly referred to as the areal density, and as described by Wallace (9) this density is directly related to the signal amplitude reproduced after the tape is used for recording purposes. Therefore, to make an advanced storage device with a volumetric density of one terabyte per cubic inch the following characteristics are required: a substrate which is approximately 4 μm thick, a magnetic medium with a track density of about 9000 tracks per inch with a 64 head array and 8 head positions, and a linear density of about 160 kbits/inch. To make a magnetic tape with such high areal densities the substrate must be mechanically and environmentally stable with a high surface smoothness. For high track densities, lateral contraction of the substrates from thermal, hygroscopic, viscoelastic, and/or shrinkage effects must be minimal. To

Table 2. List of Magnetic Tapes That Use Ultra-Thin Substrates and/or Advanced Magnetic Coatings

Magnetic Coating	Substrate	Tradename	Supplier	Thickness (μm)
ME[a]	PET	Hi8 ME-180	Sony	7.5
BaFe[b]	PET	Hi8 BaFe-120	Toshiba	11.0
ME[a]	ARAMID	NTC-90	Sony	4.8
BaFe[b]	PEN	DC2120XL	3M/Imation	7.5

[a]Metal-Evaporated Tape
[b]Barium Ferrite ($BaO \cdot 6FE_2O_3$) Particulate Coating

minimize stretching and damage during manufacturing and use of thin magnetic tapes, the substrate should be a high modulus, high strength material with low viscoelastic and shrinkage characteristics. As discussed by Bhushan (1), if the storage device is a linear tape drive, any linear deformations can be accounted for by a change in clocking speed. However, if the storage device is a rotary tape drive, anisotropic deformations of the substrate would be undesirable. To minimize stretching during use of thinner substrates, the modulus of elasticity, yield strength, and tensile strength should be high along the machine direction. Also, since high coercivity magnetic films on metal-evaporated tapes are deposited and heat treated at elevated temperatures, a substrate with stable mechanical properties up to a temperature of 100 to 150°C or even higher is desirable. In addition to mechanical and environmental stability, the cost of the material is also a major factor in the selection of a suitable substrate. Lastly, Bhushan (1) has discussed the fact that various long-term reliability problems including uneven tape-stack profiles (or hardbands), mechanical print-through, instantaneous speed variations, and tape stagger problems can all be related to the substrate's viscoelastic characteristics.

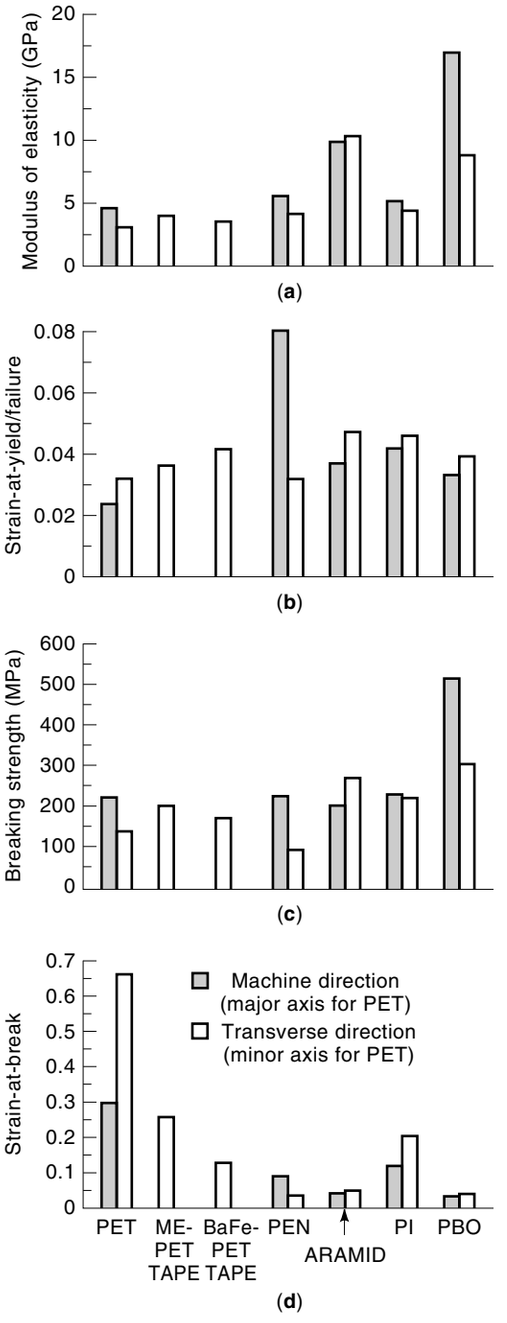

Figure 2. Mechanical properties of magnetic tape substrates [Weick and Bhushan (4)].

TENSILE PROPERTIES

Mechanical properties of typical magnetic tapes and substrates are presented in Fig. 2. These properties were measured by Weick and Bhushan (4) using a Monsanto Tensometer T20 tensile test machine in accordance with ASTM Spec. 1708. Properties presented in Fig. 2 include modulus of elasticity, strain-at-yield/failure, breaking strength, and strain-at-break. The strain-at-break measurements correspond with the strain at which the substrates break, and the strain-at-yield/failure measurements correspond with the strain at which the substrates start to deform irreversibly. Figure 2(a) shows modulus of elasticity measurements for PET, two PET tapes, and the alternative substrates. PEN, ARAMID, PI, and PBO all offer improvements in elasticity when compared to 3 to 4 GPa for PET. Elastic moduli range from 4 to 5.4 GPa for PEN, 10 GPa for ARAMID, 4 to 5 GPa for PI, and 9 to 17 GPa for PBO. The alternative substrates also offer improvements in breaking strength when compared to PET and PET tapes. Therefore, based on a typical tape tension of 7.0 MPa (1000 psi), the alternative materials would be stressed to only a fraction of their breaking strength (typically 1/10 to 1/30). Strain-at-break measurements indicate that PET tends to be more ductile than the alternative substrates. However, for PET irreversible strain occurs at its yield point. This is indicated in Fig. 2(b), and strains of only 0.02 to 0.03 were measured when PET begins to yield. The PET tapes yield at slightly higher strains of 0.03 to 0.04. PI also fails at its yield point, but PEN, ARAMID, and PBO do not have yield points. Instead, they fail irreversibly only at their breaking points. The failure strains for the alternative substrates are typically higher than those measured for PET ranging from 0.03 to 0.08 for PEN, 0.035 to 0.05 for ARAMID, 0.04 to 0.045 for PI, and 0.03 to 0.04 for PBO.

Anisotropic characteristics of the tape substrate materials are shown in Fig. 3. Modulus of elasticity measurements along different material orientations are shown in this polar plot. Since ARAMID has a circular curve, it is a relatively isotropic material with an elastic modulus of approximately 10 GPa regardless of material orientation. PI is also relatively isotropic, but its modulus is significantly less than ARAMID's. PET and PEN not only have low moduli, but they are anisotropic materials as indicated by their elliptical curves. Figure 3 also shows that even though PBO has a high modulus, it is also anisotropic.

VISCOELASTIC CHARACTERISTICS (NONPERMANENT DEFORMATION)

Time-Dependent Creep Behavior

Viscoelasticity refers to the combined elastic and viscous deformation of a polymeric material when external forces are

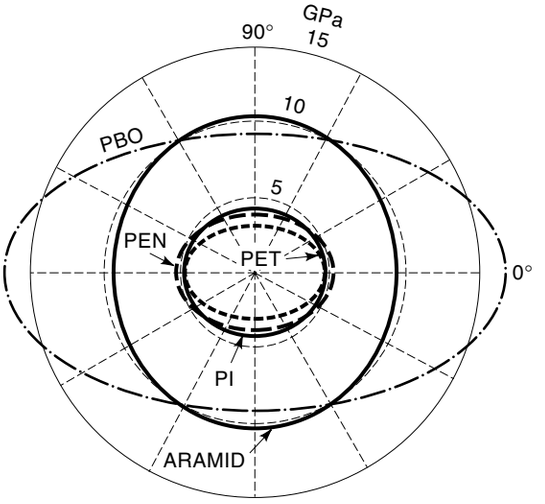

Figure 3. Anisotropy in modulus of elasticity for magnetic tape substrates. 0°—machine direction (major axis for PET); 90°—transverse direction (minor axis for PET) [Weick and Bhushan (4)].

applied. It is a function of time, temperature, and rate of deformation, and viscoelastic deformation of a magnetic tape can lead to the loss of information stored on the tape. For instance, various long-term reliability problems including uneven tape-stack profiles (or hardbands), mechanical print-through, instantaneous speed variations, and tape stagger problems can all be related to the substrate's viscoelastic characteristics. To minimize these reliability problems, it is not only important to minimize creep strain, but the rate of increase of total strain needs to be kept to a minimum to prevent stress relaxation in a wound reel.

A common method to measure time-dependent viscoelastic behavior at elevated temperatures is to perform creep experiments. Weick and Bhushan (5,6) have performed such experiments for magnetic tapes and substrates. During a creep experiment, a constant stress is applied to a strip of material (i.e., tape or substrate), and the change in length of this test sample is measured as a function of time at an elevated temperature. The amount of strain the material is subjected to can be calculated by normalizing the change in length of the specimen with respect to the original length. Creep compliance can then be calculated by dividing the time-dependent strain by the constant applied stress:

$$\epsilon(t) = \frac{\Delta l(t)}{l_0} \tag{1}$$

$$D(t) = \frac{\epsilon(t)}{\sigma_0} = \frac{\Delta l(t)}{\sigma_0 l_0} \tag{2}$$

where

$\Delta l(t) \equiv$ change in length of the test sample as a function of time
$l_0 \equiv$ original length of the test sample
$\epsilon(t) \equiv$ the amount of strain the test sample is subjected to
$\sigma_0 \equiv$ constant applied stress
$D(t) \equiv$ tensile creep-compliance of the test sample as a function of time

Typical creep-compliance measurements for magnetic tapes and substrates are shown in Figs. 4(a) and (b) for the 50 °C temperature level, and the first derivative of the creep-compliance data for the substrates is shown in Fig. 5. This first derivative represents the creep velocity of the substrates, and is a more direct depiction of the rate at which the deformation occurs. More information about how the creep velocity curves were obtained can be found in Ref. 6.

Creep-compliance data presented in Fig. 4(a) show that there is an initial creep response which occurs in the first minute of each experiment due to immediate elastic and short term viscoelastic behavior of the materials. Throughout the rest of the experiments the materials creep (or stretch) due to the viscoelastic behavior of the particular polymer being evaluated. PET shows the largest amount of creep along its

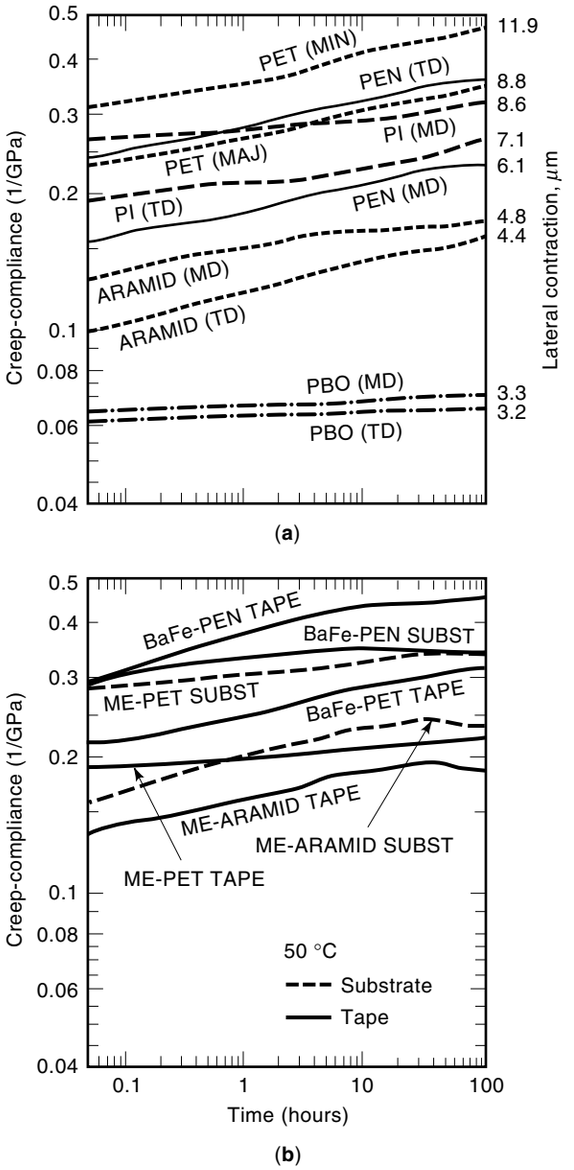

Figure 4. Creep-compliance measurements for (a) Magnetic tape substrates. The right axis shows lateral contraction calculations assuming a Poisson's ratio of 0.3 [Weick and Bhushan (5,6)]. (b) Actual magnetic tapes and their respective substrates.

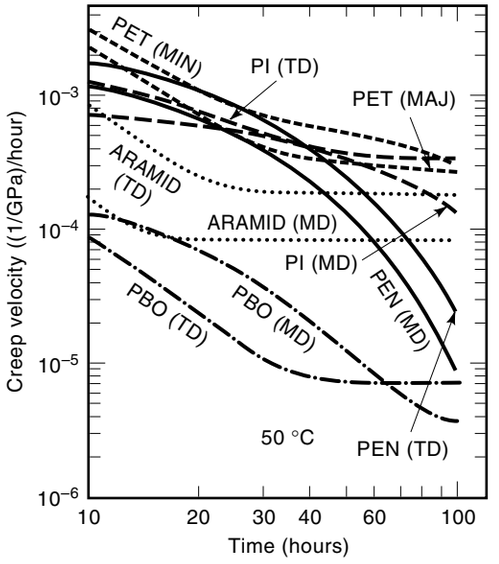

Figure 5. Creep velocity measurements for magnetic tape substrates [Weick and Bhushan (5,6)].

minor axis. PEN and PI show somewhat less creep; whereas ARAMID and PBO have total creep-compliances which are significantly lower. Creep-compliance measurements at ambient temperature show similar trends and are discussed by Weick and Bhushan (6) along with relationships between creep behavior and the molecular structure of each polymeric substrate.

From the total creep-compliance measurements at 50°C the amount of lateral contraction can be calculated as shown on the right-hand axis of Fig. 4(a). For a 12.7 mm wide tape, PET shows the largest amount of lateral contraction (approximately 12 μm along the minor axis), and PBO shows the least amount of contraction (a little more than 3 μm). PEN shows 6 to almost 10 μm of lateral contraction depending on the material orientation, whereas ARAMID shows only 4 to 5 μm.

Creep-compliance results for actual magnetic tapes are shown in Fig. 4(b). With the exception of BaFe-PET, measurements are presented for both the magnetic tapes and substrates. The substrates for the ME tapes were obtained by dipping the tapes in a 10% (vol.) HCl solution to dissolve the magnetic coating. The BaFe-PEN tape was scrubbed with methyl ethyl ketone to remove the magnetic layer and obtain the substrate. This method could not be used successfully for the BaFe-PET tape. From Fig. 4(b), the two particulate tapes (BaFe-PET and BaFe-PEN) have rates of creep which are relatively equivalent with BaFe-PEN showing a higher initial compliance. The ME-PET and ME-ARAMID tapes have lower total compliances than the particulate tapes, and the ME-ARAMID tape tends to have a higher creep velocity and lower initial compliance. When the creep behavior for each tape is compared to their respective substrate there is also an apparent difference between metal-evaporated and particulate tapes. Both ME-PET and ME-ARAMID have substrates which show a higher total creep compliance than the tape, and the creep velocity of these substrates is similar to that measured for the tapes. BaFe-PEN, on the other hand, has a substrate which tends to have a lower total creep compliance and creep velocity. This is possibly due to the presence of a lower modulus (higher compliance) elastomeric binder coating on the BaFe-PEN tape which contributes to the overall creep behavior of the composite material. Note that the thickness of the magnetic layer/coating is 3 μm and the thickness of the PEN substrate is 4.5 μm.

Creep velocity data sets are shown in Fig. 5 on a log–log scale. PBO appears to creep at the lowest rate throughout the 100 hour experiments. When compared to PET, PI offers only a slight improvement in creep velocity; whereas the creep velocity for ARAMID is always lower than the velocity for PET. During the first part of the experiment PEN creeps at a rate which is nearly equal to the creep velocity for PET. However, at the end of the experiment the creep velocity for PEN is an order of magnitude lower than the velocity for PET. PEN also creeps at a lower rate than ARAMID after 100 h.

Figure 5 not only shows relative creep rates for the materials, additional information can be extracted from the slopes of the creep velocity curves. These slopes indicate acceleration (or deceleration) during the creep process. Typically, the materials show a decreasing creep velocity and a negative slope which indicates deceleration during the creep process. For ARAMID, the slope of the creep velocity curve remains constant after 100 h. This means that ARAMID continues to creep at the same rate without a change in velocity. In comparison, PEN not only creeps at a lower rate than ARAMID after 100 h, but the changing slope of the curves for PEN indicates that the creep velocity for PEN is decreasing. Recall from Figs. 4(a) and (b) that the total creep for ARAMID is actually less than the total creep for PEN. However, from this discussion PEN actually creeps at a lower rate than ARAMID, and this rate shows a decreasing trend after 100 h.

An analytical technique known as time-temperature superposition (TTS) has been used by Weick and Bhushan (5, 6) to predict long-term creep behavior of magnetic tape substrates at ambient temperature. Using this technique creep measurements at elevated temperatures are assembled to predict behavior at longer time periods. Results are presented in Fig. 6 for the machine direction (major optical axis for PET). The trend lines (or master curves) are assembled to predict the creep-compliance at 25°C over a 10^6 h time period. Shift factors tabulated above the figure show how much each curve was shifted (in hours) to enable a smooth fit at the 25°C reference temperature. Therefore, an indication of viscoelastic behavior at very short ($<$0.1 h) and very long time periods ($>10^6$ h) can be obtained. PET and PI show similar amounts of creep until the final decades when the amount of creep for PET exceeds that for PI. PEN shows somewhat less creep at all time periods, and ARAMID has creep characteristics which are always slightly lower than PEN's. The total creep for PBO is significantly lower than that measured for the other materials.

Frequency-Dependent Dynamic Mechanical Behavior

Weick and Bhushan (10,11) have shown that the dynamic mechanical response of a magnetic tape as it is unwound from a reel and travels over a head also depends on the elastic and viscoelastic characteristics of the magnetic tape. This elastic/viscoelastic recovery and subsequent conformity of the tape with the head occurs in just a few milliseconds, and requires optimization of the dynamic properties of the materials that comprise a magnetic tape. Note that a lack of tape-to-head

conformity can lead to an increase in wear of the head as demonstrated by Hahn (12), and tape stiffness has been shown by Bhushan and Lowry (13) to be related to edge wear of a head.

Dynamic viscoelastic properties of magnetic tapes and substrates can be measured using dynamic mechanical analysis (DMA), and the information acquired from this analysis includes E' which is the storage or elastic modulus, and the lost tangent, $\tan(\delta)$, which is a measure of the amount of viscous or nonrecoverable deformation with respect to the elastic deformation. Both E' and $\tan(\delta)$ are measured as a function of temperature and deformation frequency, and results can be used to predict the dynamic response of tapes over several orders of magnitude. Equations used to calculate the storage modulus, E', and loss tangent, $\tan(\delta)$, are as follows:

$$E' = \cos(\delta)\left[\frac{\sigma}{\epsilon}\right] \tag{3a}$$

$$E'' = \sin(\delta)\left[\frac{\sigma}{\epsilon}\right] \tag{3b}$$

$$|E^*| = \sqrt{(E')^2 + (E'')^2} \tag{3c}$$

$$\tan(\delta) = \frac{E''}{E'} \tag{3d}$$

where

E' = storage (or elastic) modulus
E'' = viscous (or loss) modulus
$|E^*|$ = magnitude of the complex modulus
ϵ = applied strain
σ = measured stress
δ = phase angle shift between stress and strain

A Rheometrics RSA-II dynamic mechanical analyzer was used to measure the dynamic mechanical properties of magnetic tapes and substrates. At temperature levels ranging from −50 to 50°C, the analyzer applies a sinusoidal strain on the sample at frequencies ranging from 0.016 to 16 Hz. The strain is measured by a displacement transducer, and the corresponding sinusoidal load on the sample is measured by a load cell. Since the polymeric tapes are viscoelastic there will be a phase lag between the applied strain and the measured load (or stress) on the specimen. The storage (or elastic) modulus, E', is therefore a measure of the component of the complex modulus which is in-phase with the applied strain, and the loss (or viscous) modulus, E'', is a measure of the component which is out-of-phase with the applied strain. The in-phase stress and strain results in elastically stored energy which is completely recoverable, whereas out-of-phase stress and strain results in the dissipation of energy which is nonrecoverable and is lost to the system. Therefore, the loss tangent, $\tan(\delta)$, is simply the ratio of the loss (or viscous) modulus to the storage (or elastic) modulus. Refer to the texts by Ferry (14), Tschoegl (15), and Aklonis and MacKnight (16) for more information about polymer viscoelasticity.

Representative E' and $\tan(\delta)$ data for five substrate materials are shown in Figs. 7(a) and (b), and E' and $\tan(\delta)$ data for representative magnetic tapes are shown in Figs. 8(a) and (b). Note that these are master curves which were generated by Weick and Bhushan (10,11) using the raw E' and $\tan(\delta)$ data that are functions of both frequency and temperature. This technique is known as frequency-temperature superposition, and is analogous to the time–temperature superposition technique described for time-dependent creep behavior. A 20°C reference temperature was used for the frequency-temperature superposition, and the shift factors can be found in Refs. 10 and 11.

At the 20°C reference temperature used to construct Figs. 7(a) and (b), PET and PI show the lowest storage moduli. Note that these data sets are for the machine direction (MD), and similar results have been found by Weick and Bhushan (10) for the transverse direction (TD). However, PET clearly has the lowest E' when measured in the transverse direction. PEN, ARAMID, and PBO have significantly higher storage

Shift factors, $\log(a_T, h)$ (Reference temperature = 25 °C)

T (°C)	PET (MAJ)	PEN (MD)	ARAMID (MD)	PI (MD)	PBO (MD)
25	0	0	0	0	0
40	–2.68	–2.93	–2.20	–2.30	–1.68
50	–4.05	–3.74	–4.04	–4.88	–4.14

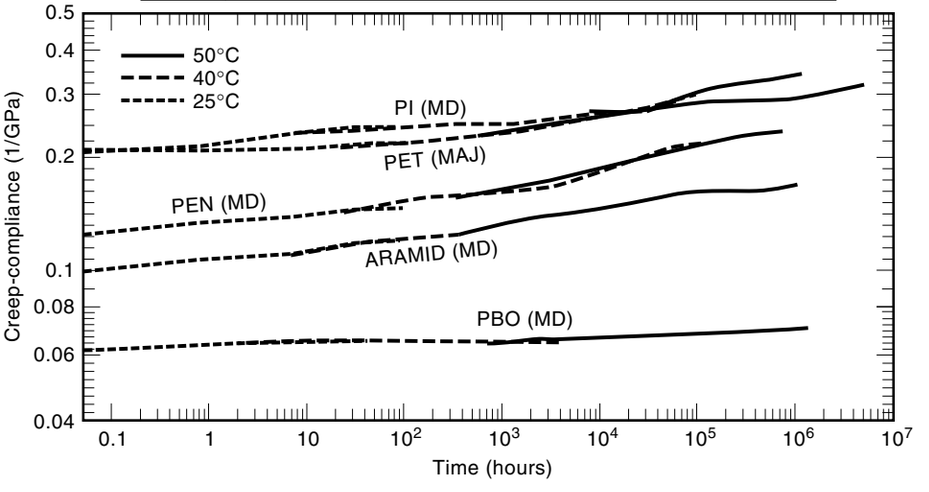

Figure 6. Creep-compliance master curves and shift factors for magnetic tape substrates. Machine direction data (major axis for PET) [Weick and Bhushan (5,6)].

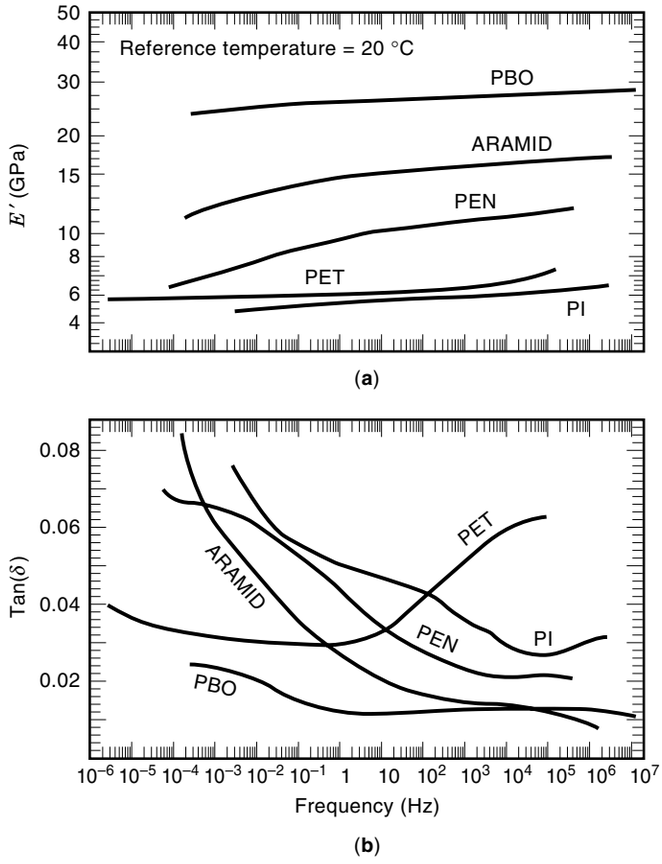

Figure 7. Typical dynamic mechanical analysis results for five magnetic tape substrates. Data sets are for PEN, ARAMID, PI, and PBO samples cut in the machine direction, and for PET samples cut along their major optical axis. [Weick and Bhushan (10)].

moduli than the other materials regardless of material orientation. Note that creep-compliance is inversely proportional to the storage modulus, and the general trends shown in Fig. 7(a) are in agreement with what is shown in Fig. 4(a). The storage modulus and tan(δ) data for PET are also in agreement with what was reported previously by Bhushan (1) for 23.4 μm thick PET substrates. The same trends have been observed but the storage moduli for the 14.4 μm thick PET are 2 to 2.5 GPa higher than what was reported by Bhushan (1), and the tan(δ) measurements are approximately 0.02 lower. These differences are not unexpected due to probable improvements in manufacturing the newer 14.4 μm thick PET material.

In general, the storage moduli for tapes made with PET substrates are lower than those measured for the tapes made with PEN and ARAMID substrates. This is shown in Fig. 8(a), and is primarily due to the fact that the more advanced PEN and ARAMID substrates have higher storage moduli than the PET substrates [Weick and Bhushan (10)]. The only exception to this is the MP-PET tape which has a somewhat higher modulus than the BaFe-PEN tape. Weick and Bhushan (11) have suggested that this could be due to the relatively thick MP film on the PET substrate which when applied to the substrate causes a more substantial increase in the modulus of the tape as a whole.

Loss tangent master curves in Figs. 7(b) and 8(b) show the relative amount of nonrecoverable, viscous deformation experienced by each substrate or tape. Recall that the loss tangent, tan(δ), is the ratio of the loss modulus, E'', to the storage modulus, E'. The storage modulus, E', is the elastic component of the modulus which responds in-phase with the applied strain, and E'' is the viscous component which lags the applied strain. Therefore, tan(δ) is the phase lag between the two components and is a relative measurement of nonrecoverable deformation. From Fig. 7(b) it can be seen that the loss tangent for all the substrates but PET shows a decreasing trend with increasing frequency. Therefore, at higher frequencies PI, PEN, ARAMID, and PBO do not dissipate as much nonrecoverable energy as PET, and PET is more likely to be deformed and stretched when it experiences high frequency transient strains in a tape drive. Similar results are shown in Fig. 8(b) for the tapes. The PET tapes show an increasing trend with increasing frequency, and the ME-ARAMID and BaFe-PEN tapes show a decreasing trend.

A complete discussion of the differences between DMA data for the tapes when compared to the substrates has been presented by Weick and Bhushan (11). To do this comparison accurately, DMA data sets were obtained for tapes and their actual constitutive substrates. To get these constitutive substrates, magnetic films and backcoatings were removed from magnetic tapes using suitable solvents [Weick and Bhushan

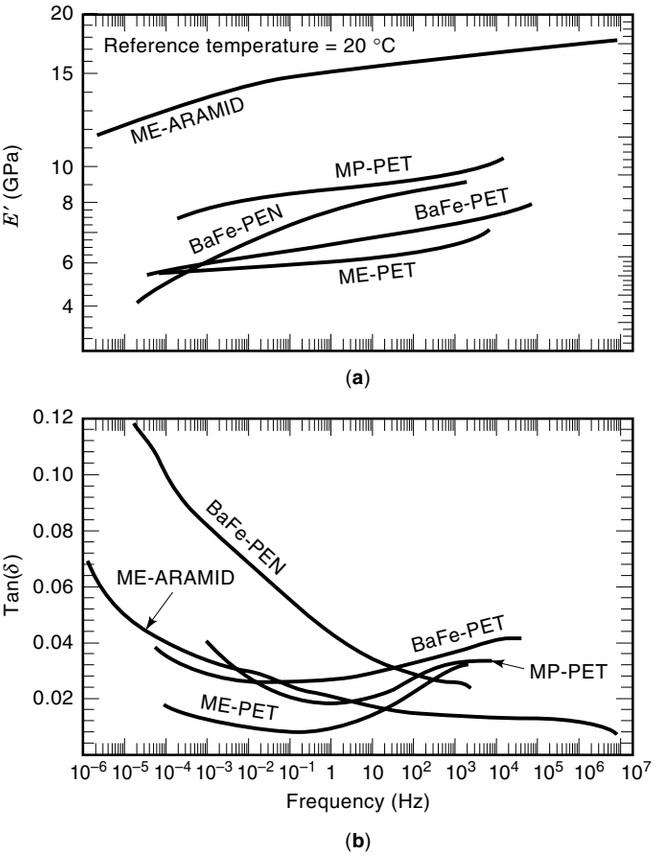

Figure 8. Dynamic mechanical analysis results for five magnetic tapes. (a) Storage modulus (E') master curves. (b) Loss tangent (Tan δ) master curves [Weick and Bhushan (11)].

(11)]. (Note that the substrates used to obtain the measurements shown in Fig. 7 were obtained directly from the polymer film manufacture, and had never been used in an actual tape.) In general, the storage modulus for a magnetic tape is typically higher than the storage modulus for its respective substrate. This is not surprising since magnetic coatings are comprised of either rigid ceramic or metal particles in an elastomeric film, or a continuous metal film. Since these magnetic films are likely to have a higher modulus than the polymeric substrates, when they are applied to the substrate the overall modulus of the composite magnetic tape is higher than the substrate alone. However, orientation, shape, and stiffness of the particles used in the magnetic coating could lead to exceptions to this general trend [Weick and Bhushan (11)].

SHRINKAGE, THERMAL, AND HYGROSCOPIC EXPANSION (PERMANENT DEFORMATION)

At elevated temperatures and humidities, polymeric materials (and therefore magnetic tapes) are susceptible to permanent deformation. One of these deformation mechanisms is known as shrinkage. Weick and Bhushan (5,6) have shown that when certain magnetic tapes (and substrates) are subjected to relatively small tensile stresses (<0.5 MPa), they tend to shrink or contract rather than creep. Shrinkage results for magnetic tape substrates are shown in Fig. 9(a). Only ARAMID (MD) and PEN (MD & TD) shrink at this temperature level. PEN shrinks as much as 0.035% after 100 h, and ARAMID (MD) shrinks 0.01% after 100 h. The relatively large amount of shrinkage for PEN could be reduced by stress-stabilizing the material at 65°C. Creep appears to be a more dominant factor for PET since its change in length is positive rather than negative. The effect of polymeric structure and processing conditions on substrate shrinkage behavior can be found in Ref. 6.

Shrinkage measurements have also been obtained for the magnetic tapes. These results are presented in Fig. 9(b). BaFe-PET initially creeps and then shrinks in a manner which is similar to that observed for a 14.4 μm thick PET substrate. The ME-PET tape shrinks considerably more (0.03% after 100 h), and the ME-PET substrate shrinks 0.05%. This could mean that there are residual stresses present in the ME-PET substrate which are somewhat attenuated when the metal coating is applied. The ME-ARAMID tape and substrate shrink in a manner which was already observed for the ARAMID (MD) substrate evaluated separately (see Fig. 9(a)). Since the substrate shrinks less than the tape, residual stresses may have actually been added when the metal coating was applied.

Certain magnetic tape materials also undergo free expansion when subjected to elevated temperatures and humidities. Coefficient of thermal expansion (CTE) and coefficient of hygroscopic expansion (CHE) measurements have been reported by Weick and Bhushan (4), and are shown in Figs. 10(a) and (b). CTE measurements were made in accordance with ASTM D696-79 using a Zygo laser dimension sensor. Specimens cut into 13 × 1/2 inch strips were used for CTE, and the temperature was varied from 24 to 46°C. CHE measurements were made using a Neenah paper expansimeter. The humidity was varied from 27–95% using a salt solution, and 5 × 1/2 inch specimens were used. ARAMID and PEN have lower thermal

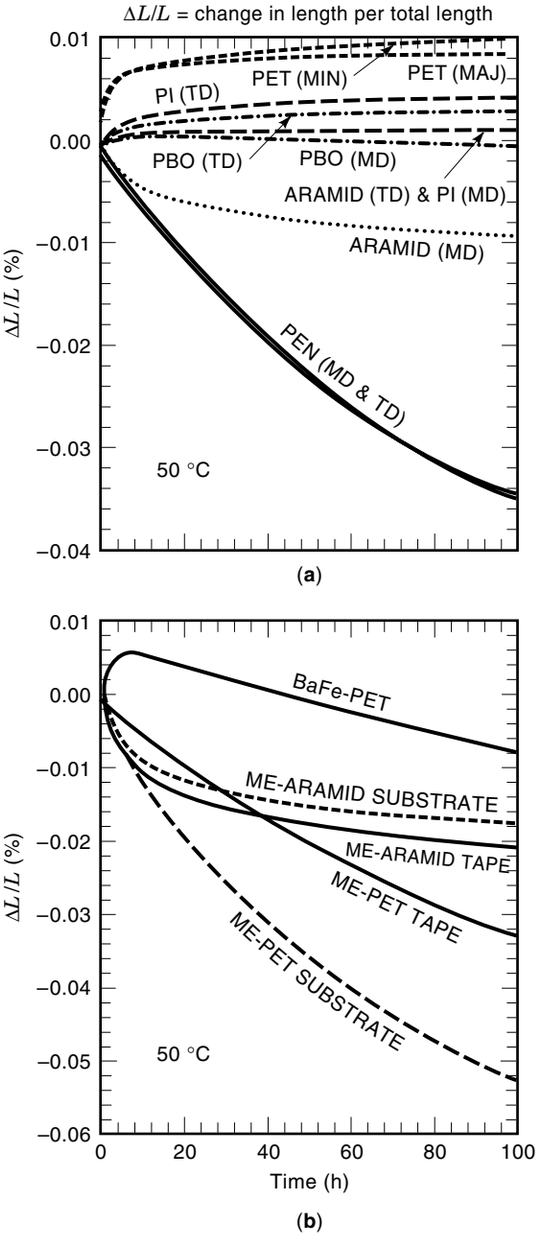

Figure 9. Shrinkage measurements for (a) Magnetic tape substrates. (b) Actual magnetic tapes and their respective substrates [Weick and Bhushan (5,6)].

expansion characteristics than PET. However, only ARAMID and PBO show a significant decrease in hygroscopic expansion. See Perettie et al. (17), Perettie and Pierini (18), and Perettie and Speliotis (19) for additional information.

A summary of the deformation characteristics measured for magnetic tape substrate materials by Bhushan (1), Weick and Bhushan (4), and Perettie and Pierini (18) is presented in Table 3, and CTE, CHE, creep, lateral contraction, and shrinkage measurements are presented on a percentage basis in Fig. 11. ARAMID and PEN both offer improved expansion and contraction characteristics when compared to PET. Although these materials shrink slightly more than PET at 50°C, their expansion and contraction characteristics are lower.

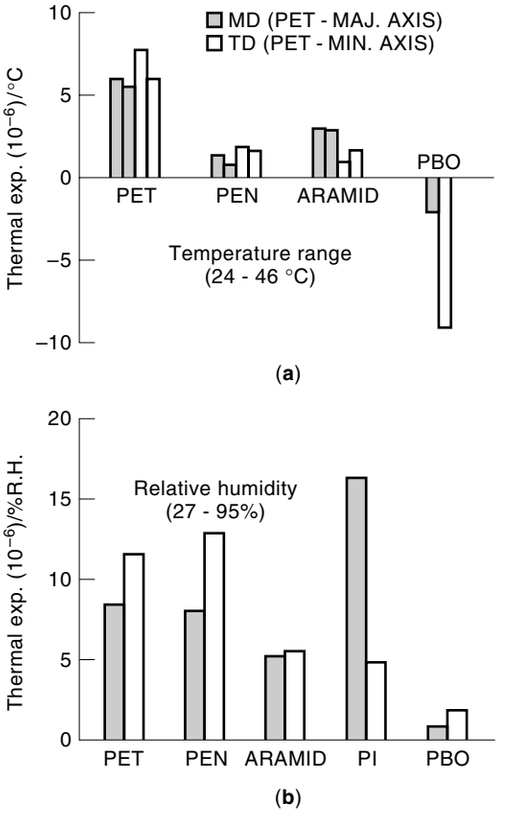

Figure 10. Thermal and hygroscopic expansion measurements for magnetic tape substrates. MD is the machine direction (major axis for PET), and TD is the transverse direction (minor axis for PET) [Weick and Bhushan (4)].

Weick and Bhushan (1,6) have reported that the shrinkage for PEN and polyesters in general could be reduced by stress-stabilizing the material at 65°C. ARAMID and PEN are also closer to the contraction criteria for an advanced magnetic tape with 256 tracks per inch to be read at a time. Based on this criteria lateral contraction should be less than 0.08% if a 1/10 track mismatch is tolerable and the head can be recentered. It is not entirely clear whether ARAMID or PEN should be used for the next generation of magnetic tapes. However, ARAMID has a higher T_g than the polyester films, which makes it more suitable for metal evaporated tapes. Also, the elastic modulus is a factor of two higher for ARAMID when compared to PEN, and ARAMID is more isotropic which renders it more compatible with rotary tape drives. PEN on the other hand has a creep velocity shown in Fig. 5 which is lower than that for ARAMID, and the creep velocity for PEN continues to decrease after 100 h at 50°C. In comparison, ARAMID continues to deform viscoelastically at the same rate. See Refs. 5 and 6 for more information about creep velocity.

Although other substrates such as PBO and ARAMID clearly offer advantages over PET and PEN, it should be noted that PET is still the standard substrate used for magnetic tapes. PBO and PI have not been used due to their lack of availability and high cost. ARAMID is also a high cost material since it is manufactured using a casting technique rather than the drawing technique used for the polyester films (PET and PEN). PEN is now being used in place of PET for certain long-play video tapes as well as higher density data storage tapes such as the 3M DC2120XL, and ARAMID is used as the substrate for the Sony NTC-90 microcassette. A final ranking of substrates can be made based on the summaries presented in Table 3 and Fig. 11: 1st choice—PBO (unavailable), 2nd choice—PEN or ARAMID, 3rd choice—PI (availability in question), 4th choice—PET.

TRIBOLOGICAL CHARACTERISTICS

Surface Roughness

Roughness of the substrates is a concern when higher areal densities are required. The substrate must have a high surface smoothness in addition to being mechanically and environmentally stable. Furthermore, for the advanced magnetic tapes such as metal-evaporated (ME) tape, the surface of the substrate must be tailored to allow for the deposition and adhesion of thin metal coatings. Surface topography is also an important parameter which influences handling of the substrate. Throughout manufacture, conversion, and use Bhushan (1) has reported that the film must be able to be wound at high speeds without stagger (lateral slip) in the transverse direction. During winding it is necessary for each layer to tighten and cinch upon itself. To insure stability in the layer-

Table 3. Summary of Mechanical, Hygroscopic, Thermal, Viscoelastic, and Shrinkage Characteristics of Magnetic Tape Substrates

Material		Mod. of Elasticity (GPa)	Strain at Yield/ Failure	Breaking Strength (MPa)	Strain at Break	Density g/cm³	Moist. Absorb.[a] (%)	CHE (27–95%) (10^{-6})/%RH	CTE (24–46°C) (10^{-6})/°C	T_g (°C)	Melting Point (°C)	Creep-Compl. 100 hrs @ 50°C (GPa^{-1})	Lat. Contract.[b] 100 hrs @ 50°C (μm)	Shrinkage 100 hrs @ 50°C (%)
PET	MAJ	4.3	0.02	221	0.29	1.395	0.4	8.5	6.0	116	263	0.35	9.3	neg.
	MIN	2.9	0.03	141	0.66			11.7	7.9			0.47	12.5	
PEN	MD	5.4	0.08	222	0.08	1.355	0.4	8.1	1.5	156	272	0.23	6.1	0.034
	TD	4.1	0.03	298	0.03			12.9	1.9			0.36	9.6	0.034
ARAMID	MD	9.8	0.04	200	0.04	1.500	1.5	5.3	3.1	277	None	0.18	4.8	0.011
	TD	10.2	0.05	271	0.05			5.5	1.0			0.16	4.3	neg.
PI	MD	4.8	0.04	227	0.12	1.420	2.9	13.0	—	360–410	None	0.33	8.6	neg.
	TD	4.2	0.05	223	0.21			—	—			0.27	7.1	
PBO	MD	16.8	0.03	511	0.03	1.540	0.8	1.0	−2.0	—	None	0.069	1.84	neg.
	TD	8.8	0.04	305	0.04			2.0	−9.0			0.067	1.79	

[a]24 hrs at 22 °C. [b]Calculated from creep-compliance data for a 12.7 mm wide substrate using a Poisson's ratio of 0.3 and applied stress of 7.0 MPa.

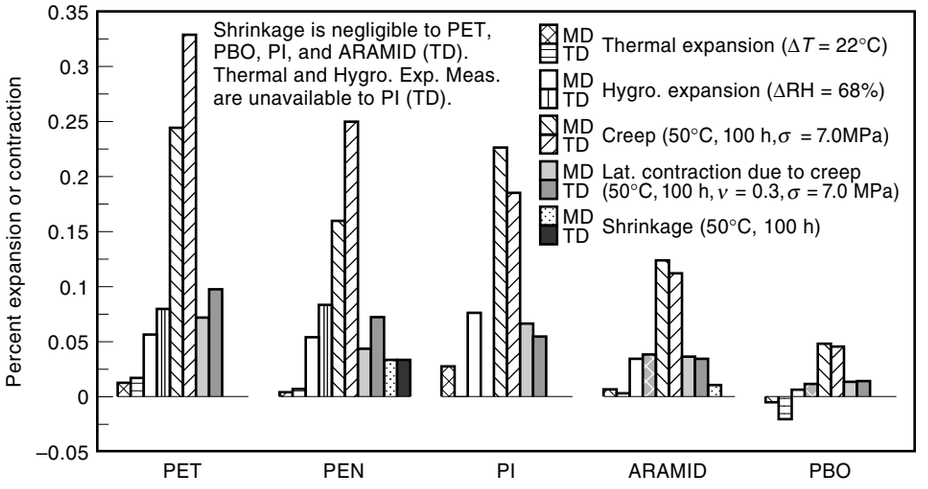

Figure 11. Summary of expansion and contraction characteristics for magnetic tape substrates where the data has been reduced to a percentage scale [Weick and Bhushan (4)].

to-layer contact, Bhushan (1), Bhushan and Koinkar (20), and Oden et al. (21) have reported that particles known as "anti-slip" agents are commonly dispersed in PET before extrusion. The presence of these particles also affects the abrasion of the PET film (unbackcoated tape surface) when it is in sliding contact with tape drive components or during winding or spooling.

Surface roughness profiles are shown in Fig. 12 for the magnetic tape substrates. These profiles were taken using a commercially available atomic force microscope (AFM), and the scan size was set to 100 × 100 μm. Root-mean-square (rms) roughness values are tabulated in this figure along with peak-to-valley (P–V) and peak-to-mean (P–M) distance measurements for each substrate. The roughness profile for PET indicates that anti-slip particles are present in the polymer. These particles ensure that the substrate can be wound tightly on to itself, and prevent any layer-to-layer slippage between wraps. Typically, two size distributions of particles are used: submicron particulates with a height of approx. 0.5 μm to reduce interlayer friction, and larger particles with a height of approximately 2 to 3 μm to control the air film (Bhushan (1) and Bhushan and Koinkar (20)). The larger particles are typically composed of ceramics such as silica, titania, bentonite, calcium carbonate, or clays of different kinds. Bhushan (1) has discussed the fact that these particles are known to affect the abrasion resistance of the PET film (unbackcoated tape surface) when used in sliding contact with components in a tape drive or during winding on the spool.

The surface of the alternative substrate PEN is substantially smoother than the surface of PET. Furthermore, the P–V and P–M distance values for PEN are less than half that for PET indicating that anti-slip agents are not present in PEN. ARAMID also has a substantially lower rms than PET and PEN. The rms for ARAMID is 10.6 nm compared to 37.2 nm for PET and 15.8 nm for PEN. P–V and P–M distance values for ARAMID are less than 1/3 that measured for PET and half that measured for PEN. PI offers the smoothest topography with an rms of 3.20 nm; however the P–V and P–M values for PI are higher than that for ARAMID possibly due to imperfections in the surface. PBO has an rms of 16.5 nm which is similar to that measured for PEN, but the P–V and P–M values for PBO are much lower indicating that PBO has fewer surface imperfections.

In addition to the 100 × 100 μm scans, 10 × 10 μm AFM scans were also performed. Results are summarized for both scan sizes in Table 4. With the exception of ARAMID and PI, rms roughness decreases with scan size as reported by Bhushan and Ruan (22). This is also true for P–V and P–M with the exception of ARAMID. Therefore, in general, smaller regions of the substrates appear to be smoother, and the probability of hitting a significantly high peak decreases with scan size. ARAMID is the exception, rms doubles, and P–V and P–M increase slightly. This increase in rms is most likely indicative of a surface modification performed on ARAMID to accommodate metal-evaporated coatings.

Friction

Since magnetic recording devices require low motor torque and high magnetic reliability, the finished magnetic medium must also exhibit low friction/stiction and high durability. Interlayer friction between a substrate and itself is important since the substrate must be wound onto itself during manufacturing. Similarly, interlayer friction between an unbackcoated tape (the substrate) and a coated magnetic tape is important during actual tape drive operation since an unbackcoated side of a tape will be in contact with a coated tape surface during reel winding. In addition, for unbackcoated tapes the substrate can contact tape path components directly. Therefore, friction between the substrate and these components is important, and ferrite is typically chosen as the countersurface for tribological studies [Bhushan and Koinkar (20)].

Friction measurements have been made by Weick and Bhushan (10) using a reciprocating friction tester (REFT). For these experiments a 12.7 mm wide by 270 mm long substrate strip was drawn back and forth over a countersurface at a constant velocity of 25 mm/s for each pass. The applied stress was 7.0 MPa and the duration of the experiments was 15 min. Three different countersurfaces were utilized for the friction experiments: (1) a Ni–Zn ferrite tape head (IBM 3480/3490-type, rms = 2.2 nm, P–V distance = 21 nm), (2) a sample of the substrate itself, and (3) a metal particle tape (MP-tape) with an rms roughness of 5.7 nm and peak-to-valley distance of 56 nm. Three to four repeats were performed for each sub-

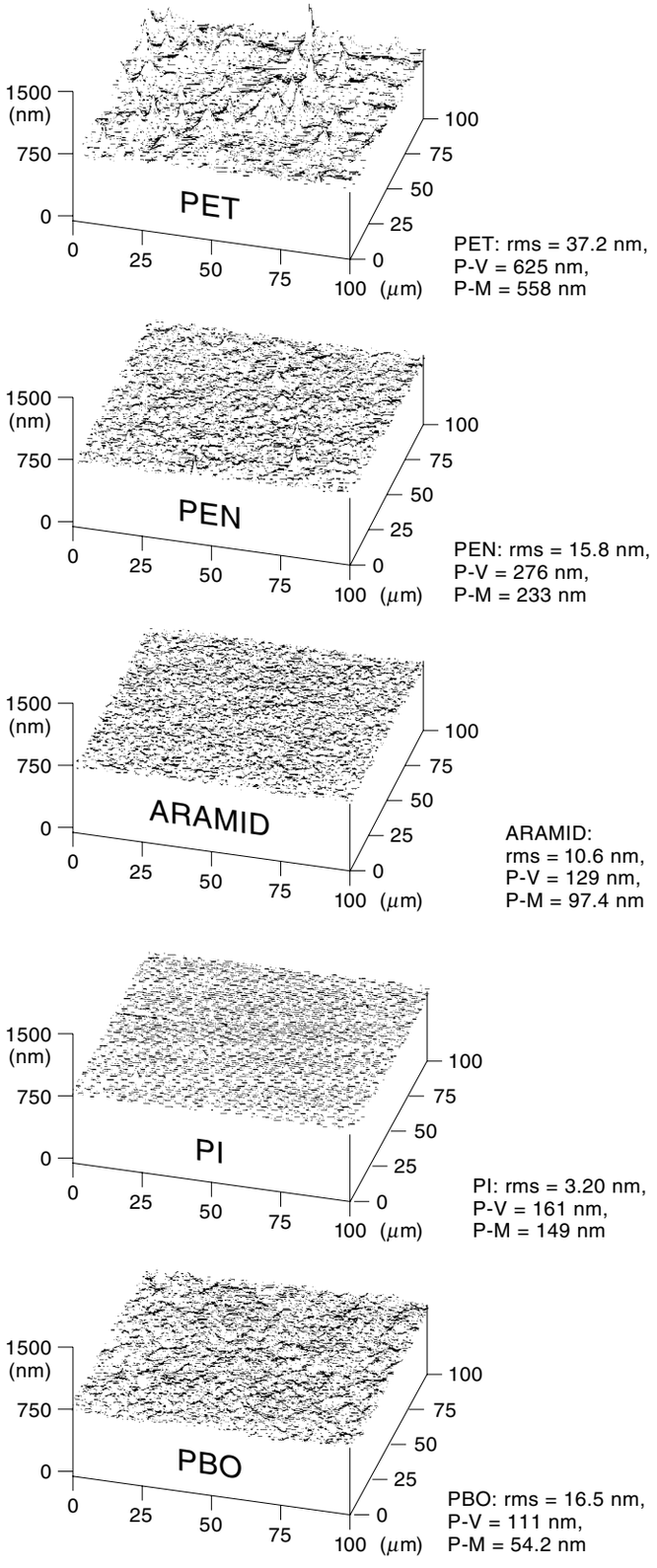

Figure 12. Surface roughness profiles for magnetic tape substrates (100×100 μm^2 AFM scans). Root mean square (rms) roughness values are shown along with peak-to-valley (P–V) and peak-to-mean (P–M) roughness values [Weick and Bhushan (10)].

strate, and the average peak friction was calculated for each pass along with the 95% confidence intervals.

Friction measurements are tabulated in Table 4 along with 95% confidence intervals. Friction traces are shown in Fig. 13. For PET, higher friction coefficients were measured when the substrate was rubbed against itself or an MP tape than when it was rubbed against a ferrite surface. A similar trend was found by Bhushan and Koinkar (20), but lower friction coefficients were measured in the present study possibly due to the newer 14.4 μm PET (Mylar A DB grade) substrate used in this research. The higher friction coefficient measured when PET was rubbed against itself could be attributed to higher plowing contributions from the interaction of the antislip particles. Furthermore, the MP tape used in this study has an rms roughness of 5.7 nm versus 2.2 nm for the ferrite surface. Therefore, plowing interactions between antislip agents in the PET substrate and asperities on the relatively rough MP tape surface could lead to higher friction. When PET is rubbed against the ferrite surface there is less plowing, and the harder, higher modulus ceramic antislip particles could lead to a lower real area of contact, lower frictional forces, and a lower adhesive friction component.

For PEN, higher friction coefficients were measured when it was rubbed against a ferrite surface than when it was rubbed against itself or an MP tape countersurface. This is the opposite trend to what was observed for PET. Note that PEN has a lower rms roughness and P–V distance than PET due to a lack of hard, ceramic, antislip particles. Therefore, due to the lack of these particles, the adhesive friction component will be lower and the friction coefficient for PEN rubbing against ferrite will be higher. The PEN substrate could also form larger real areas of contact with the head leading to higher adhesive friction forces. Furthermore, in keeping with concepts presented by Fowkes (23,24), *acidic* groups in the polyester backbone of PEN can interact and adhere more readily with the *basic* ferrite surface which is comprised of various oxides (11% NiO, 22% ZnO, 67% Fe_2O_3). Friction coefficients measured against itself and MP tape are also higher for PEN versus PET although the confidence intervals are rather high. This could be attributed to more asperities interlocking with the countersurface leading to an increase in the plowing component. Although the particles on a PET surface are large and will indeed interact, the total summation of the areas which are interlocking could be smaller for PET versus PEN.

The friction trend for ARAMID is similar to that observed for PEN: friction against ferrite is higher than against itself or MP tape. Since the structure for ARAMID contains the relatively acidic amide linkages, acid-base interactions with the basic ferrite surface is again more likely. Although this is not indicated in Table 4 by the lower friction coefficient of 0.49 ± 0.06 for ARAMID versus 0.59 ± 0.06 for PEN, the trend line in Fig. 13 shows that the confidence interval for ARAMID is large at the beginning and the end of the experiment. Electrostatic attraction between ARAMID and the head was also more pronounced than for the other materials, and could play a role along with acid-base interactions. Frictional effects for ARAMID against itself and the MP tape are also lower when compared to the same measurements for PET. Since the rms, P–V, and P–M are significantly lower for ARAMID than for

Table 4. Coefficient of Friction and Surface Roughness Measurements for Magnetic Tape Substrates

	Surface Roughness—Atomic Force Microscope Measurements								
	Scan Size: 100 × 100 μm			Scan Size: 10 × 10 μm			Coefficient of Friction for Substrate		
Substrate	Rms (nm)	Pk-Valley (nm)	Pk-Mean (nm)	Rms (nm)	Pk-Valley (nm)	Pk-Mean (nm)	Against Ni–Zn Ferrite	Against Itself	Against MP Tape
PET	37.2	625.	558.	16.1	147.	116.	0.29 ± 0.02	0.39 ± 0.02	0.41 ± 0.10
PEN	15.8	276.	233.	10.8	126.	105.	0.59 ± 0.06	0.47 ± 0.02	0.47 ± 0.09
ARAMID	10.6	129.	97.4	20.2	142.	101.	0.49 ± 0.06	0.21 ± 0.05	0.27 ± 0.10
PI	3.20	161.	149.	3.76	35.8	24.8	—	—	—
PBO	16.5	111.	54.2	9.99	66.1	32.2	0.43 ± 0.01	0.43 ± 0.07	0.45 ± 0.18

PET (based on 100 × 100 μm AFM scans), frictional effects due to plowing could be lower for ARAMID. Although the rms roughness for ARAMID increases to 20.2 nm (versus 16.1 nm for PET) when a 10 × 10 μm scan size is used, a reduction in plowing is still felt to be a feasible explanation for the lower ARAMID - ARAMID and ARAMID - MP tape friction. This is due to the fact the friction measurements are macroscopic in nature and should be compared to large scale roughness measurements such as the 100 × 100 μm AFM scans.

There is no significant difference in friction measurements for PBO when it is rubbed against ferrite, itself, or an MP tape. Although PBO has an rms which is approximately equal to PEN's, its P–V and P–M values are significantly lower. Therefore, plowing contributions from interlocking asperities are not likely to be present when PBO is rubbed against itself or an MP tape. Furthermore, since PBO does not contain the acidic groups present in ARAMID and PEN, there is no measurable increase in friction when it is rubbed against a basic ferrite countersurface. However, friction is slightly higher for PBO when compared to PET. No concrete explanation for this can be made, but PBO does have a significantly higher tensile strength than PET, and it is likely to have a higher shear strength, which would lead to an increase in the friction based on a simple adhesion model.

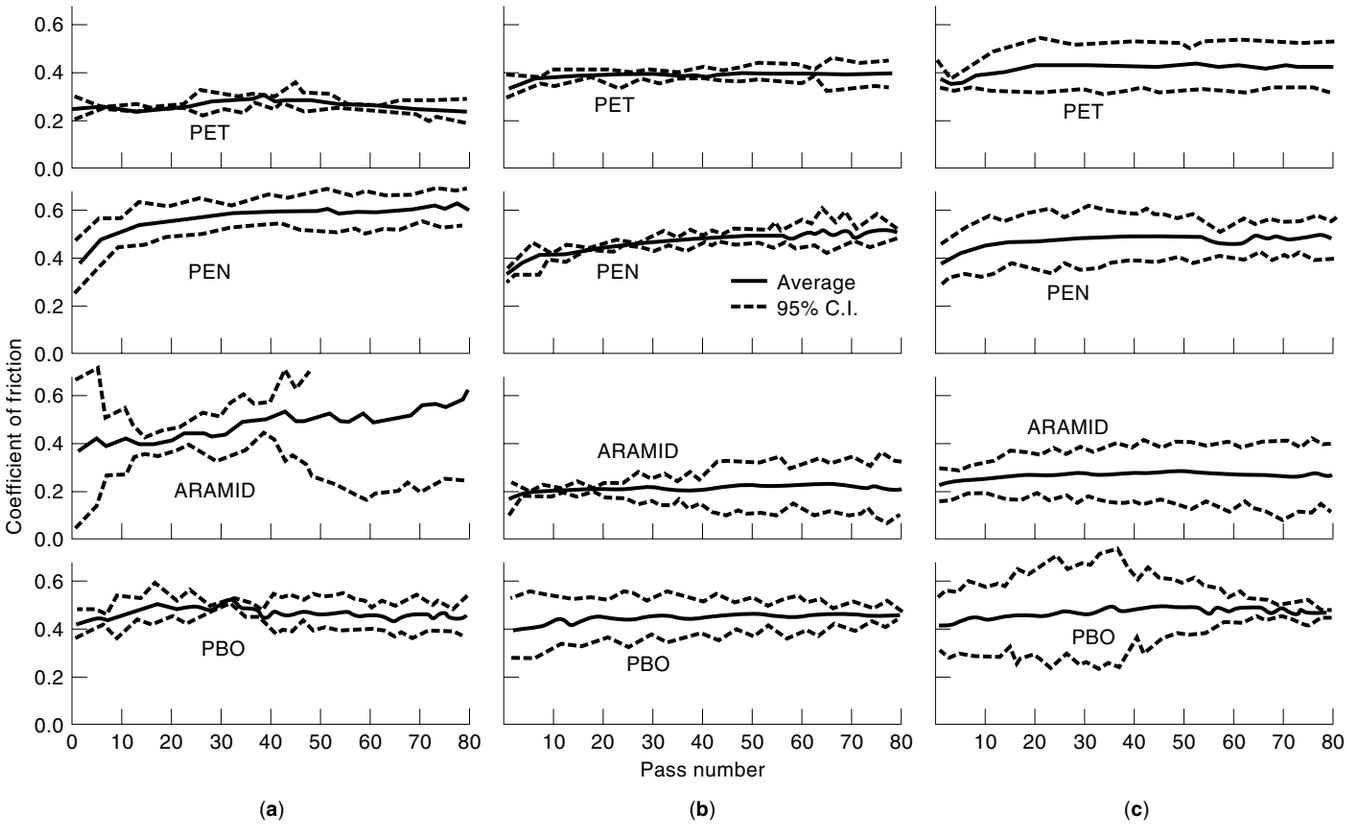

Figure 13. Friction measurements for magnetic tape substrates rubbing against (a) A Ni–Zn ferrite head, (b) Themselves, and (c) An MP tape. The velocity = 25.4 mm s^{-1}, sample length = 270 mm, applied stress = 7.0 MPa, and the duration of the experiments = 15 min [Weick and Bhushan (10)].

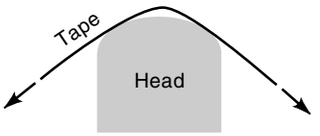

Figure 14. Schematic drawing of a tape traveling over a head and forming two distinct contact regions due to lack of tape-to-head conformity [Weick and Bhushan (10)].

MECHANICAL DESIGN CONSIDERATIONS

Tape-to-Head Conformity and Dynamic Tape–Head Interactions

Typically, a high modulus substrate is desirable for a magnetic tape during fabrication and use of the tape. Bhushan (1) and Weick and Bhushan (4,5) have shown that high modulus, high strength films such as PEN, ARAMID, or PBO are more desirable to minimize stretching and damage of the tape and subsequent loss of information stored on the tape. However, Hahn (12) has found that there is a direct relationship between head wear and bending stiffness of a magnetic tape. Since bending stiffness is proportional to the product of modulus and moment of inertia, it is clear that higher modulus substrates can lead to increased head wear. This increasing relationship is attributed to a lack of tape-to-head conformity. Stiffer, higher modulus tapes will form contact zones as shown schematically in Fig. 14.

From the creep and DMA studies performed by Weick and Bhushan (4–6,10,11) using magnetic tapes and substrates, it is clear that a viscoelastic tape substrate material has a temperature and frequency-dependent modulus. Therefore, under certain circumstances in a tape drive the modulus of a tape substrate will increase and affect the tape-to-head conformity. Two of these circumstances are discussed by Weick and Bhushan (10) using a PEN substrate as an example. The first circumstance is referred to as Case 1, and it considers the deformation frequency for a perturbation in the tape as it comes off a roll (or bearing) near the head. When this occurs the segment can experience a perturbation which propagates at a velocity ΔV. This propagation velocity is related to the tape tension and mass density of the tape [Stahl et al. (25)].

$$\Delta V = \sqrt{\frac{T}{m}} \tag{4}$$

where

T = the applied tape tension in the drive
m = the linear mass density of the tape in kg/m

From Fig. 15 the frequency of this velocity disturbance, f_{d1}, is inversely related to the time it takes for a tape segment to travel from the roll at $x = 0$ to the head at $x = L$. Therefore, f_{d1} is equal to ΔV divided by the distance L:

$$\text{Case 1}: \qquad f_{d1} = \frac{\Delta V}{L} = \frac{1}{L}\sqrt{\frac{T}{m}} \tag{5}$$

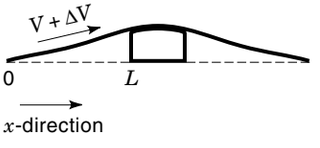

Figure 15. Diagram of a tape traveling from a roll or bearing at $x = 0$ to the head $x = L$ [Weick and Bhushan (10)].

For a 3480/3490-type head, the distance L is approximately equal to 20 mm. The typical axial stress applied to a tape is 7.0 MPa. Using a 4.5 μm thick PEN substrate as an example, the tension is 0.40 N for a 12.7 mm wide tape substrate. Since the linear mass density for PEN is $7.3(10^{-5})$ kg/m, f_{d1} is 3.71 kHz from Eq. (5).

The other circumstance, Case 2, considers the deformation frequency when a tape substrate encounters and travels over the head. This second deformation frequency is directly related to the fact that the tape does not immediately form a stable hydrodynamic air film. The sudden change in curvature associated with the tape bending over the head together with such factors as the air film viscosity, velocity of the tape, and tension per unit width all contribute to the deformation of the tape over a finite arc distance along the head. The coordinate for this distance is s, and a tape segment encountering the head will undergo a change in height, Δh_0, which is a maximum at the air film entrance region, and will become zero when a stable air film of thickness h_0 is formed. This change in height is due to the increase in pressure from ambient to the pressure associated with the hydrodynamic air film. Gross (26) has presented the following equations to calculate the ratio $\Delta h(s)/h_0$:

$$\frac{\Delta h(s)}{h_0} = Ae^{-\xi} \tag{6a}$$

$$\xi = \frac{s\epsilon^{1/3}}{h_0} \tag{6b}$$

$$\epsilon = \frac{6\mu V}{T/w} \tag{6c}$$

where

$\Delta h(s)$ = change in the thickness of the hydrodynamic air film as a function of s
h_0 = thickness of the stable air film
s = longitudinal coordinate along the head
A = a constant which is typically exceedingly small (23)
μ = the dynamic viscosity in $\text{N} \cdot \text{s/m}^2$
V = the average tape velocity in m/s
T/w = the tape tension per unit width of tape in N/m

Equations (6a–c) are only true at the entrance region to the head and can be used to predict the distance s_1 through which the tape is subjected to the transient deformation. Since the change in thickness of the air film is a function of h_0 as well as the other variables already listed, curves can be drawn for various h_0 values which show $\Delta h/h_0$ as a function of s. These curves are shown in Fig. 16, and $\Delta h/h_0$ has been divided by the unknown constant A. The initial height of the deformation is governed by the magnitude of this constant. The distance s_1 can be found from the point at which each of the curves reaches a $\Delta h/Ah_0$ of zero. However, since the functions shown in Eq. 6(a–c) are exponential functions that decrease asymptotically and therefore never truly reach zero, s_1 will be se-

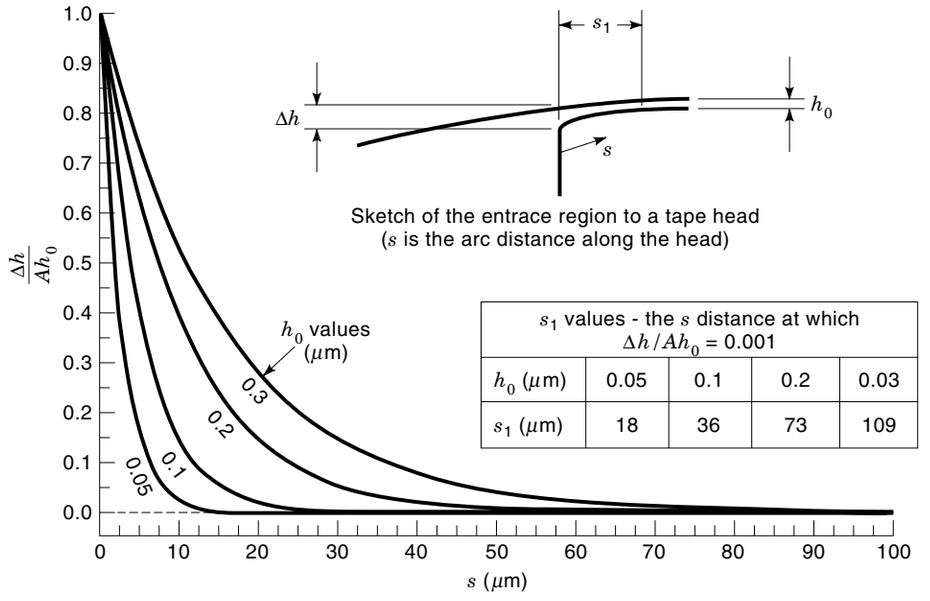

s_1 values - the s distance at which $\Delta h/Ah_0 = 0.001$				
h_0 (μm)	0.05	0.1	0.2	0.03
s_1 (μm)	18	36	73	109

Figure 16. Variation in air-bearing thickness at the entrance region (Δh) as a function of stable film thickness values h_0. Curves are for a PEN substrate, similar curves can be developed for other substrates and tapes [Weick and Bhushan (10)].

lected at the point where $\Delta h/Ah_0$ is 0.1% of its maximum value of 1. Once s_1 is found Eq. (7) can be used to calculate a second deformation frequency using the average tape velocity, V:

$$\text{Case 2}: \qquad f_{d2} = \frac{V}{s_1} \tag{7}$$

From Fig. 16, s_1 is equal to 36 μm for an h_0 of 0.1 μm which is a typical value for the thickness of the stable air film between a tape and an IBM 3480/3490-type head (Bhushan (1)). For an average velocity, V, of 2 m/s the frequency, f_{d2}, is equal to 56 kHz.

To determine the deformation strain, the frequency-dependent storage modulus from DMA master curves such as the those shown in Figs. 7(a) or 8(a) can be used together with the maximum stress in the tape, σ_{max}. The following equation gives an estimate of the strain as a function of deformation frequency where f_d is equal to either f_{d1} or f_{d2}:

$$\epsilon(f_d) = \frac{\sigma_{\max}}{E'(f_d)} \tag{8}$$

Although Eq. (8) shows that ϵ and E' are functions of frequency, it should be understood that these parameters are also functions of temperature.

In Eq. (8) σ_{max} is equal to either σ_{max1} or σ_{max2} depending on whether Case 1 or 2 is being used to determine how the tape is deformed. σ_{max1} is the axial stress on the tape as it travels from the roll to the edge of the head, and σ_{max2} is the stress on the tape as it travels over the head. Therefore, the equation for σ_{max2} considers the fact that the tape is not only subjected to an axial tensile stress, it is also subjected to a bending stress from the head. Although the tape is flexible and can be slowly wrapped around objects such as the head without exceeding its stress limit, Bhushan (1) and Hahn (12) have reported that when the tape is used in a high-speed tape drive it will act like a stiff, rigid member at high deformation rates. Equations and derivations for σ_{max1} and σ_{max2} can be found in Ref. 10.

For both Cases 1 and 2 the storage modulus will increase as a function of frequency as shown in Figs. 7(a) and 8(a). These frequency-dependent modulus values are shown in Table 5 for magnetic tape substrates as calculated using the techniques discussed by Weick and Bhushan (10). For both cases, PET and PI clearly have the lower storage moduli followed by PEN, ARAMID, and PBO. Based on the direct relationship between head wear and bending stiffness measured by Hahn (12), tapes manufactured with the lower modulus substrates such as PET or PI will potentially conform to the head more readily than PEN, ARAMID, or PBO, and wear of the head will be less for PET or PI. However, this assumes that the substrates are all of equal thickness. Since bending stiffness is directly proportional to the product of elastic modulus and the moment of inertia, thinner tapes will have a substantially lower bending stiffness even though their modulus is higher. This is because the moment of inertia for a rectangular cross-section is proportional to the cube of the thickness.

Transverse Curvature Due to Anisotropy

Recent studies by Bhushan and Lowry (13) have shown that under certain conditions there can be a higher amount of wear at the edges of a tape head when compared to the center. More specifically, the amount of edge wear relative to the wear at the center of the head is higher. This higher relative edge wear has also been shown to be related to tape stiffness, and could correspond with the edges of the tape contacting the head. Furthermore, due to the multilayer composite structure of the tape, it is likely that the tape will show transverse curvature when an axial load is applied. This transverse curvature results in a lack of transverse conformity as shown in Fig. 17. The amount of this curvature depends on the relative thickness of the layers as well as the material properties of each layer. To evaluate the extent of this transverse curva-

Table 5. Calculated Stresses and Strains Imposed on a Tape Substrate When a "Loose" Tape Segment Comes Off a Roll (Case 1), and Stresses and Strains on the Substrate Due to Deformations from Encountering the Tape Head (Case 2).[a]

			Deformation Frequencies and Stress–Strain Calculations for Case 1.				Deformation Frequencies and Stress–Strain Calculations for Case 2[b]					Tensile Test Measurements	
Substrate	Thickness. (μm)	Mass Density (10^{-4} kg/m)	f_{d1} (kHz)	E' @ f_{d1} (GPa)	σ_{max1} (MPa)	ϵ @ f_{d1}	s_1 (μm)	f_{d2} (kHz)	E' @ f_{d2} (GPa)	σ_{max2} (MPa)	ϵ @ f_{d2}	Strength (MPa)	Strain at Yield/failure
PET	23.4	4.21	3.51	6.75	7.0	0.001	63	32	7.1	22.2	0.003	220	0.05
PET	14.4	2.56	3.54	6.75	7.0	0.001	53	38	7.2	27.9	0.004	221	0.02
PEN	4.5	0.73	3.71	11.0	7.0	0.0006	36	56	11.3	52.9	0.005	222	0.08
ARAMID	4.4	0.83	3.43	16.2	7.0	0.0004	36	56	16.9	53.8	0.003	200	0.04
PI	7.6	1.40	3.48	6.25	7.0	0.001	43	47	6.4	39.5	0.006	227	0.04
PBO	5.0	1.01	3.29	27.5	7.0	0.0003	37	54	28.0	49.0	0.002	511	0.03

[a]Applied stress = 7.0 Mpa; width of substrates = 12.7 mm. Tensile test measurements are included for comparison. Calculations shown below are for a PEN substrate and an IBM 3480/3490-type head.
[b]h_o = 0.1 μm.

ture, classical lamination theory (CLT) has been used by Weick and Bhushan (11) to determine stress-strain and stiffness relationships for each layer and the composite magnetic tape as a whole. See Jones (27) for more information about CLT and mechanics of composite materials.

A material with such properties as PET is usually referred to as an orthotropic material, and the orthotropy ratio, α, is defined as the modulus along the major (or stiff) axis with respect to the modulus along the minor (or compliant) axis. PEN also has a tendency to have orthotropic characteristics; whereas a substrate such as ARAMID tends to have isotropic characteristics for which the modulus is the same regardless of material orientation. As already demonstrated in this paper, the magnetic layer will have different modulus characteristics depending on if it is a metal-evaporated (ME) film or a particulate coating (BaFe or MP). The ME film can be considered as a continuous film with isotropic characteristics. Although the particulate MP or BaFe coatings are themselves composites comprised of an elastomeric binder with hard metal or ceramic particles, Weick and Bhushan (11) modeled them as being macroscopically isotropic.

Using CLT, it can be shown that when a load per unit width, N_x, is applied to the tape, the tape will stretch, contract, and curve in the transverse direction. The analytical expression that describes this phenomenon is defined as follows:

$$N_x = A_{11}\epsilon_x + A_{12}\epsilon_y + B_{11}\kappa_x + B_{12}\kappa_y \tag{9}$$

where

$N_x \equiv$ axial force per unit width
A_{11} and $A_{12} \equiv$ stiffness terms for the axial and transverse strains, respectively

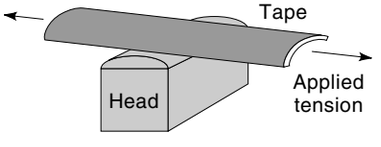

Figure 17. Lack of tape-to-head transverse conformity [Weick and Bhushan (11)].

B_{11} and $B_{12} \equiv$ stiffness terms for the axial and transverse curvatures, respectively
ϵ_x and $\epsilon_y \equiv$ strains in the x and y directions
κ_x and $\kappa_y \equiv$ curvatures in the x and y directions

Note that B_{12} is the transverse curvature stiffness, which is a measure of the tapes resistance to curvature when a load per unit width, N_x, is applied to the tape. Although it would be desirable to calculate κ_y and determine explicit numbers for the amount of transverse curvature a tape is subjected to under an axial load, this is not plausible since it would require the determination of all the stiffnesses, and a knowledge of the other strains and curvatures. Therefore, the simple approach is to calculate B_{12} from equations defined by the classical lamination theory for a two- layer composite (i.e., magnetic tape). From Eq. (9) it should be clear that higher B_{12} values correspond with lower curvatures, κ_y. Therefore, B_{12} as calculated using the equation below can be thought of as a measure of the tapes resistance to transverse curvature. Or, stated another way, tapes with higher B_{12} values will transversely conform to the head, and the edge wear phenomenon observed by Bhushan and Lowry (13) will be minimal. Since it is desirable to develop a nondimensionalized measurement of a tapes resistance to transverse curvature, B_{12} will be divided by B_0, which is defined as the B_{12} value for the tape when the magnetic film thickness is zero:

$$\frac{B_{12}}{B_0} = 1 - \left(\frac{v_a(\alpha - v_{b12}^2)}{v_{b12}(1 - v_a^2)}\right)\left(\frac{E_a}{E_{b1}}\right)\left(\frac{a}{b}\right)^2 \tag{10}$$

where

v_a and $v_{b12} \equiv$ Poisson's Ratios for the coating and substrate, respectively
E_{b1} and $E_{b2} \equiv$ elastic moduli for the major and minor axes of the substrate, respectively
$E_a \equiv$ elastic modulus for the magnetic coating
a and $b \equiv$ thicknesses of the magnetic coatings and substrates, respectively
$\alpha \equiv$ orthotropy ratio for the substrate, (E_{b1}/E_{b2})

From Eq. (10), as the thickness ratio a/b increases, the value of B_{12}/B_0 decreases. Similarly, B_{12}/B_0 will also decrease with

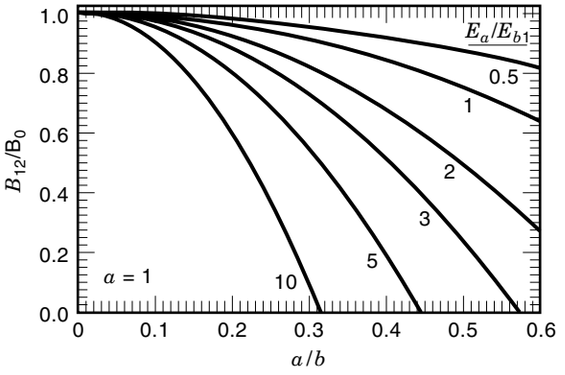

Figure 18. Transverse stiffness of magnetic tapes as a function of the thickness ratio, a/b (Poisson's ratios are assumed to be equal to 0.3). [Weick and Bhushan (11)].

an increasing modulus ratio E_a/E_{b1}, or an increasing orthotropy ratio α. Note that even if $\alpha = 1$, there will still be some curvature which will increase as a/b increases. Also, B_0 itself is a function of the orthotropy ratio. Therefore, a substrate with a high α will have a low B_0 value, and will experience some transverse curvature when an axial tension per unit width is applied.

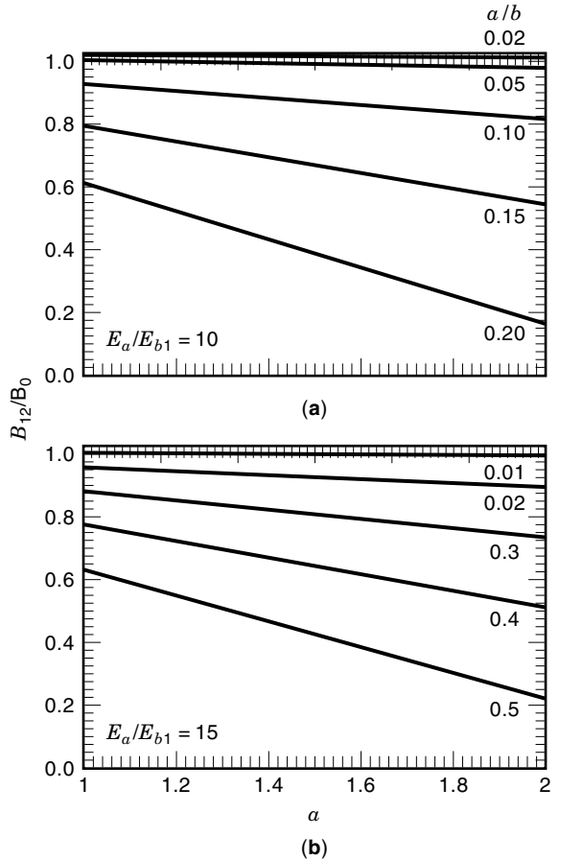

Figure 19. Transverse stiffness of magnetic tapes as a function of substrate orthotropy, α (Poisson's ratios are assumed to be equal to 0.3). [Weick and Bhushan (11)].

Figures 18 and 19 show the transverse stiffness trends for magnetic tapes in a nondimensional, graphical form. In Fig. 18, B_{12}/B_0 is shown as a function of the thickness ratio for various values of the modulus ratio. A higher thickness or modulus ratio will cause the transverse stiffness to decrease. In other words, as the thickness and/or modulus of the magnetic coating increases relative to the thickness or modulus of the substrate, the transverse curvature of the tape will increase. Note that the effect of orthotropy is not considered in Fig. 18 since the orthotropy ratio for the substrate, α, is assumed to be 1.

Figure 19 shows the effect of orthotropy on transverse stiffness for two modulus ratios. The E_a/E_{b1} ratio of 10 was used to generate the top graph in Fig. 19 and is a typical value for ME tapes; whereas the modulus ratio of 1.5 used for the bottom graph is indicative of particulate tapes such as the MP and BaFe tapes. As expected, Fig. 19 shows that as the orthotropy of the substrate increases, the transverse curvature of the tape will increase. The extent of this curvature will be greater for particulate tapes than ME tapes since the thickness ratios are typically larger for particulate tapes. Thickness ratios for the particulate tapes used in this study typically range from 0.4 to 0.6, and a/b ratios for the ME tapes are substantially smaller ranging from 0.02 to 0.04. Therefore, from Fig. 19 ME tapes with modulus ratios on the order of 10 will have B_{12}/B_0 values approaching 1. In comparison, particulate tapes will have lower transverse stiffness values ranging from only 0.2 to 0.6. As a result, tapes like ME-ARAMID will have minimal transverse curvature, and will transversely conform to the head. This will lead to minimal edge grooving of the head such as that observed by Bhushan and Lowry (13).

Critical Tension for Tape Flyability

Due to the projected use of advanced substrates for magnetic tapes, Weick and Bhushan (10) have used an experimental

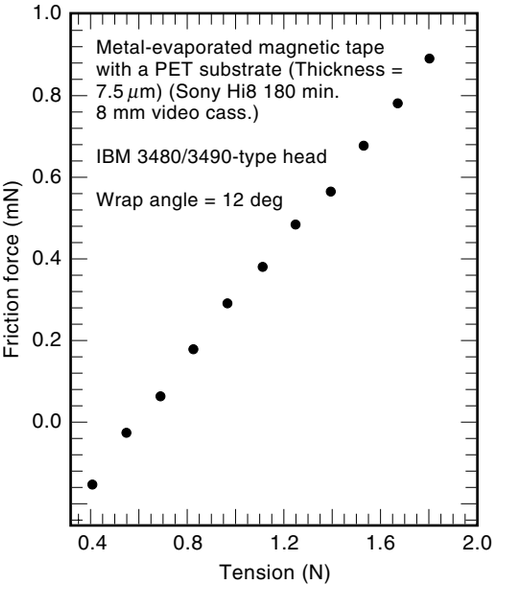

Figure 20. Relationship between friction force and tape tension. Measurements were made using a modified Honeywell Ninety Six vacuum controlled tape drive. The tape speed was 1.5 m s^{-1}, and friction forces are averages for 600 m of tape [Weick and Bhushan (10)].

technique to measure the critical tension required to maintain tape flyability and prevent overstressing of the tape. In this work, a 7.5 μm thick, 8 mm wide, metal-evaporated magnetic tape (Sony Hi-8 ME-180) was used in a Honeywell "Ninety-Six" vacuum controlled tape drive which was modified by Bhushan and Lowry (13) to accept 3480/3490-type heads. Friction forces could be measured using a split I-beam, and tension could be controlled by adjusting the vacuum pressure. Experiments were performed at different tensions, and friction forces were measured as shown in Fig. 20. Although it was expected that the friction would reach a low threshold value indicative of a complete loss of the tape-to-head air bearing, this was not observed. Instead, as tension was reduced, frictional forces between the tape and head were also reduced in a linear fashion. The limit of 0.42 N (1.5 oz) corresponded to a loss of vacuum pressure, and no visible or measurable translation of the tape, or catastrophic loss of the air bearing was observed. Furthermore, it is interesting to note that the 0.42 N limit is equivalent to a 7.0 MPa applied stress on the 7.5 μm thick magnetic tape. Although the results shown in Fig. 20 do not provide a direct solution to the question of a critical tension for the alternative substrates, they do provide an indication that frictional forces do tend to decrease with tension, and lower tensions are potentially feasible in advanced tape drives.

BIBLIOGRAPHY

1. B. Bhushan, *Mechanics and Reliability of Flexible Magnetic Media.* New York: Springer-Verlag, 1992.
2. B. Bhushan, *Tribology and Mechanics of Magnetic Storage Devices.* 2nd ed., New York: Springer-Verlag, 1996.
3. B. Bhushan, Tribology of the head-medium interface, in C. Denis Mee and Eric D. Daniel (eds.), *Magnetic Recording Technology,* 2nd ed., New York: McGraw-Hill, 1996.
4. B. L. Weick and B. Bhushan, Characterization of magnetic tapes and substrates, *IEEE Trans. Magn.,* **32**: 3319–3323, 1996.
5. B. L. Weick and B. Bhushan, Shrinkage and viscoelastic behavior of alternative substrates for magnetic tapes, *IEEE Trans. Magn.,* **31**: 2937–2939, 1995.
6. B. L. Weick and B. Bhushan, Viscoelastic behavior and shrinkage of ultra-thin polymeric films, *J. Appl. Polymer Sci.,* **58**: 2381–2398, 1995.
7. A. Feurstein and M. Mayr, High vacuum evaporation of ferromagnetic materials—a new production technology for magnetic tapes. *IEEE Trans. Mag.,* **MAG-20**: 51–56, 1984.
8. K. H. Harth et al., *J. Mag. Soc. Jpn.,* **13**(S-1): 69–72, 1989.
9. R. L. Wallace, The reproduction of magnetically recorded signal, *Bell Syst. Tech. J.,* **30**: 1145–1173, 1951.
10. B. L. Weick and B. Bhushan, The tribological and dynamic behavior of alternative magnetic tape substrates, *Wear,* **190**: 28–43, 1995.
11. B. L. Weick and B. Bhushan, The relationship between mechanical behavior, transverse curvature, and wear of magnetic tapes, *Wear,* **202**: 17–29, 1996.
12. F. W. Hahn, Wear of recording heads by magnetic tape, in B. Bhushan, et al. (eds.), *Tribology and Mechanics of Magnetic Storage Systems,* Park Ridge, IL: ASLE, **1** (SP-16): 41–48, 1984.
13. B. Bhushan and J. A. Lowry, Friction and wear studies of various head materials and magnetic tapes in a linear mode accelerated test using a new nano-scratch wear measurements technique, *Wear,* **190**: 1–15, 1995.
14. J. D. Ferry, *Viscoelastic Properties of Polymers,* 3rd. ed., New York: Wiley, 1980.
15. N. W. Tschoegl, *The Phenomenological Theory of Linear Viscoelastic Behavior: an Introduction,* New York: Springer-Verlag, 1989.
16. J. J. Aklonis and W. J. MacKnight, *Introduction to Polymer Viscoelasticity,* New York: Wiley, 1983.
17. D. Perettie et al., *J. Mag. Magn. Mat.,* **120**: 334–337, 1993.
18. D. Perettie and P. Pierini, Advanced substrates for high performance flexible media, in D. Speliotis (ed.), *Advances in Applied Magnetism, Vol I: Barium Ferrite and Advanced Magnetic Recordings.* Amsterdam: Elsevier, October 1997.
19. D. Perettie and D. Speliotis, *J. Mag. Soc. Jpn.,* **18** (S1): 279–282, 1994.
20. B. Bhushan and V. N. Koinkar, Microtribology of PET films, *Trib. Trans.,* **38**: 119–127, 1995.
21. P. I. Oden et al., AFM imaging, roughness analysis and contact mechanics of magnetic tape and head surfaces, *ASME J. Tribol.,* **114**: 666–674, 1992.
22. B. Bhushan and J. Ruan, Atomic-scale friction measurements using friction force microscopy: Part II—application to magnetic media, *ASME J. Tribol.,* **116**: 389–396, 1994.
23. F. M. Fowkes, Role of acid-base interfacial bonding in adhesion, *J. Adhes. Sci. Tech.,* **1**: 7–27, 1987.
24. F. M. Fowkes, Acid-Base interactions in polymer adhesion, in J. M. Georges (ed.), *Microscopic Aspects of Adhesion and Lubrication, Tribology Series 7.* Amsterdam: Elsevier, 119–137, 1982.
25. K. J. Stahl, J. W. White, and K. L. Deckert, Dynamic response of self-acting foil bearings, *IBM J. Res. Develop.,* **18**: 513–520, 1974.
26. W. A. Gross, *Fluid Film Lubrication.* New York: Wiley, 1980.
27. R. M. Jones, *Mechanics of Composite Materials.* New York: Hemisphere, 1975.

BRIAN L. WEICK
University of the Pacific
BHARAT BHUSHAN
Ohio State University

MAGNETIC THIN-FILM DEVICES.

See MAGNETIC MICROWAVE DEVICES.